

# Deformation of the Batestown till of the Lake Michigan lobe, Laurentide ice sheet

Jason F. THOMASON,\* Neal R. IVERSON

*Department of Geological and Atmospheric Sciences, Iowa State University, Ames, Iowa 50011, USA  
E-mail: thomason@isgs.uiuc.edu*

**ABSTRACT.** Deep, pervasive shear deformation of the bed to high strains (>100) may have been primarily responsible for flow and sediment transport of the Lake Michigan lobe of the Laurentide ice sheet. To test this hypothesis, we sampled at 0.2 m increments a basal till from one advance of the lobe (Batestown till) along vertical profiles and measured fabrics due to both anisotropy of magnetic susceptibility and sand-grain preferred orientation. Unlike past fabric studies, interpretations were guided by results of laboratory experiments in which this till was deformed in simple shear to high strains. Fabric strengths indicate that more than half of the till sampled has a <5% probability of having been sheared to moderate strains (7–30). Secular changes in fabric azimuth over the thickness of the till, probably due to changing ice-flow direction as the lobe receded, indicate that the bed accreted with time and that the depth of deformation of the bed did not exceed a few decimeters. Orientations of principal magnetic susceptibilities show that the state of strain was commonly complex, deviating from bed-parallel simple shear. Deformation is inferred to have been focused in shallow, temporally variable patches during till deposition from ice.

## 1. INTRODUCTION

Numerous authors have suggested that soft-bedded glaciers can move primarily by widespread shearing of their beds over thicknesses exceeding several decimeters (e.g. Alley and others, 1987; MacAyeal, 1992; Jenson and others 1995; Boulton, 1996b; Clark and Pollard, 1998; Licciardi and others, 1998). This mechanism of basal motion may help instigate and sustain fast glacier flow, with associated effects on ice-sheet stability and climate (e.g. MacAyeal, 1992; Clark, 1994; Clark and others, 1999). High rates of basal sediment transport (Alley, 1991; Hooke and Elverhøi, 1996; Dowdeswell and Siegert, 1999; Anandakrishnan and others, 2007) and a wide variety of glacial landforms, including some drumlins, end moraines, Rogen moraines and boulder pavements, have been attributed to this style of movement (e.g. Boulton, 1987; Clark, 1991; Hindmarsh, 1998a,b; Johnson and Hansel, 1999).

The vast basal till sheets (commonly >10 000 km<sup>2</sup>) of Wisconsin episode mid-latitude ice sheets are thought by some to have been transported by this mechanism (Alley, 1991; Clark, 1997). Others believe that, although these tills were deformed locally, they were transported largely in ice and deposited through lodgment (e.g. Clayton and others, 1989; Piotrowski and others, 2001), the process whereby debris is released from sliding basal ice and accumulates on the bed. Both processes undoubtedly involve shear of basal sediments, but the bed-deformation model, through its requirement that most basal motion occur by simple shear of the bed, must result in ratios of bed-surface displacement to shearing-bed thickness (bed shear strains) in excess of 100, even for slow glaciers (10 m a<sup>-1</sup>), short occupation times (100 years) and thick shear zones within the bed (5 m). The bed-deformation model also requires that strain in the

bed extend to depths greater than those associated with deformation caused by particle ploughing during lodgment. Deformation depths due to ploughing are conservatively one to five times the particle diameter, as indicated by wedge and cone-penetration studies (Baligh, 1972, 1985; Koumoto and Kaku, 1982), and are likely proportional to the coarseness of particles that constitute the bed (Tulaczyk, 1999; Thomason and Iverson, 2008). Thus, given the small volume fraction of cobbles and boulders in many tills, deformation depths due to ploughing and lodgment should not generally exceed a few decimeters.

Testing the bed-deformation model using basal tills of the geologic record therefore requires evidence that allows inconsequential shear strains (<<100) to be distinguished from the higher strains of the model. Additional evidence should distinguish shallow deformation of the bed from deep deformation to high strains. Also, evidence that sheds light on the three-dimensional state of strain in the bed should be sought to try to establish that bed-parallel simple shear dominated strain.

Developing definitive testing criteria is difficult. Qualitative descriptions of till micromorphological features from many studies (see Menzies and others, 2006, for a review) indicate that basal tills have commonly been deformed, but to strains that are poorly known. Macroscopic heterogeneities in till can provide indicators of strain direction and magnitude but are expected to be homogenized at the high strains required of the bed-deformation model (e.g. Clark, 1997; Piotrowski and Tulaczyk, 1999; Van der Wateren and others, 2000), so the magnitude of deformation of commonly massive tills is unclear. The degree of particle mixing at till contacts has been used to demonstrate bed deformation (Carlson and others, 2004; Piotrowski and others, 2004) but has not generally yielded quantitative estimates of strain magnitude, despite the potential for such estimates (Hooyer and Iverson, 2000b). Efforts to assign unique particle-fabric signatures to 'deformation tills' and 'lodgment

\*Present address: Illinois State Geological Survey, 615 East Peabody Drive, Champaign, Illinois 61820, USA.

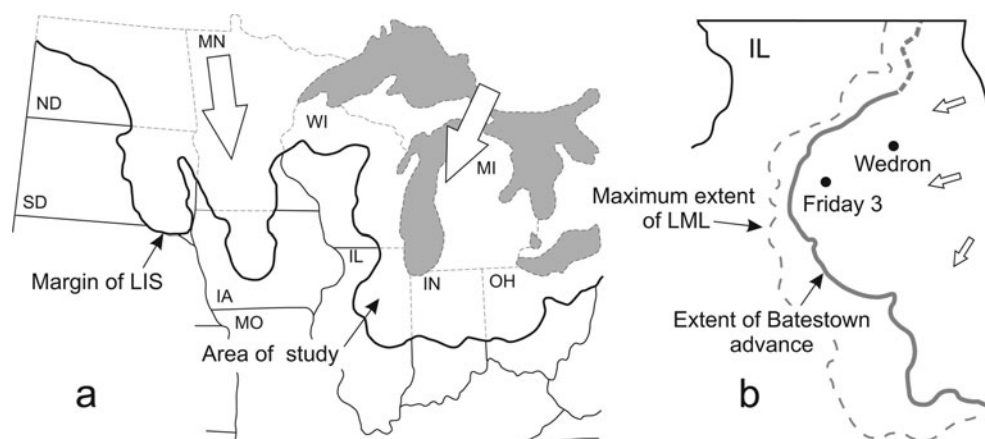


**Fig. 1.** (a) Study area and late-Wisconsin southern margin of the Laurentide ice sheet (LIS). (b) Locations of Friday 3 and Wedron exposures, with maximum extent of the Lake Michigan lobe (LML) and footprint of the Batestown advance in Illinois.

tills' are viewed with increasing skepticism owing to unresponsive field data (Bennett and others, 1999) and appreciation that both facies involve similar styles of shear (Evans and others, 2006; Iverson and others, 2008). Partly as a result of these ambiguities, the lack of consensus regarding basal-till transport mechanisms is striking. For example, note the strongly contrasting reviews of Boulton and others (2001) and Piotrowski and others (2001) regarding the importance of bed deformation in sediment transport.

The goal of this study was to evaluate whether the Batestown till, a basal till deposited by a late-Wisconsin advance of the Lake Michigan lobe of the Laurentide ice sheet (Fig. 1), deformed in a manner consistent with the bed-deformation model. Such deformation has been suggested for this till by several authors (Jenson and others, 1995, 1996; Boulton, 1996a; Johnson and Hansel, 1999). Our approach is different from past ones in that our interpretations are guided by results from experiments in which the Batestown till was sheared to high strains (Thomason and Iverson, 2006; Hooyer and others, 2008; Iverson and others, 2008). These experiments indicate that the state of strain of this till can be estimated from two types of till particle fabric that can be measured with high spatial resolution: fabrics formed by principal directions of magnetic susceptibility and fabrics formed by orientations of sand-grain long axes. We summarize these experimental results and then use them to interpret the state of strain in the Batestown till from magnetic and particle fabrics measured in densely sampled profiles in northern Illinois. Resultant quantitative constraints on the magnitude, style and depth of bed deformation provide criteria for evaluating aspects of the bed-deformation hypothesis.

## 2. BACKGROUND

### 2.1. Till fabric

Grains rotate in till during its deformation, resulting in partial alignment of the long axes of non-equant grains to form a fabric. Fabric strength and direction should be related to the three-dimensional state of strain in the till, ideally as expressed by a second-rank tensor (Oertel, 1996). Till-fabric characteristics have also been related to the geomorphic context (e.g. Boulton, 1976; Benn, 1995; Yi and Cui, 2001), till-layer thickness (Hart, 1994, 1995; Hart and Rose, 2001)

and the degree to which till may have displayed fluid-like behavior, as indicated by its porosity, water content or strength (Dowdeswell and others, 1985; Benn, 1995, 2002; Benn and Evans, 1996; Evans and others, 2006). However, the state of cumulative strain, by directly influencing grain rotation, is the most obvious first-order control on fabric, as emphasized by structural geologists interested in preferred clast orientations in rocks (Nicolas, 1992; Tikoff and Teyssier, 1994) and fault gouge (Cladouhos, 1999).

There is widespread but not universal agreement that high cumulative strains in till result in strong pebble fabrics parallel to the direction of shear (Benn, 1995; Benn and Evans, 1996; Piotrowski and others, 2001; Carlson and others, 2004; Evans and others, 2006). This relationship is supported by experiments in which till containing pebbles was sheared to known strains and fabric development was measured (Hooyer and Iverson, 2000a). These experiments also showed that steady fabric strengths were attained at moderate shear strains ( $\sim 20$ ), and provided no support for the postulate that particles in shearing till assume transverse or poorly aligned orientations at sufficiently high strains (e.g. Clark, 1997; Lian and others, 2003; Hart, 2006). Such transverse or weak fabrics at high strains are expected from the model of Jeffery (1922), but slip of matrix grains across the surfaces of pebbles in till clearly violates the no-slip condition of the Jeffery theory. This slip at the surfaces of pebbles, as indicated by their commonly striated surfaces (e.g. Benn, 2002), keeps them aligned in the direction of shear (Hooyer and Iverson, 2000a; Iverson and others, 2008).

There are several problems with using pebble fabrics. The relatively low density of pebbles in many tills, including the Batestown till, limits the spatial resolution of pebble fabrics to zones in the bed that may be thicker than zones where shear deformation occurred (Hooyer and others, 2008). Human subjectivity and error in measuring pebble fabrics are well documented (Drake, 1977; Klein and Davis, 2002). Perhaps most importantly, little useful information is contained in the orientations of the intermediate and short axes of pebbles; they provide, for example, no information about the three-dimensional state of strain.

Two other kinds of till fabric measurements are also made: fabrics formed by directions of maximum magnetic susceptibility in intact till specimens (Fuller, 1962; Gravenor and others, 1973; Stupavsky and others, 1974; Gravenor and

Stupavsky, 1975; Boulton, 1976; Eyles and others, 1987; Stewart and others, 1988; Principato and others, 2005) and those formed by the long axes of sand particles measured in thin section (e.g. Ostry and Deane, 1963; Evenson, 1971; Yi and Cui, 2001; Carr and Rose, 2003). These studies have yielded important insights regarding till genesis, but until recently the relationship between fabric characteristics and the magnitude and direction of strain had not been demonstrated. Ring-shear experiments with basal tills, including the Batestown till, have provided this relationship for the case of simple shear (Thomason and Iverson, 2006; Hooyer and others, 2008; Iverson and others, 2008) and hence serve as a rational basis for interpreting our field measurements.

## 2.2. AMS and sand fabrics caused by simple shear: past experimental results

The Iowa State University ring-shear device shears a water-saturated till specimen that is ~75 mm thick. Shearing speeds are glacial ( $10\text{--}800\text{ ma}^{-1}$ ), and effective normal stresses are similar to those measured beneath glaciers ( $5\text{--}400\text{ kPa}$ ). The rotary design and associated annular specimen chamber place no limit on strain magnitude. Deformation within the central  $10\text{--}35\text{ mm}$  of the till specimen is relatively uniform and closely approximates simple shear. Specimens for fabric analysis are collected from within this zone, so the distribution of strain outside this zone, which reflects lateral boundary effects (Iverson and others, 1997), is irrelevant (Thomason and Iverson, 2006). Prior to an experiment, wet till is mixed in the specimen chamber to minimize preferred particle orientation. Consolidation of the specimen by  $\sim 5\text{--}15\%$ , after application of the normal stress, causes discernible but minimal preferred orientation of sand grains (e.g. Thomason and Iverson, 2006) and of axes of maximum magnetic susceptibility (Hooyer and others, 2008). The till is then sheared to a predetermined displacement. Shear strain is calculated as the shearing displacement along the specimen center line divided by the shear-zone thickness, which is indicated by the relative displacement of marker beads that spanned the shear zone.

On completion of experiments conducted to various shear strains, intact till samples are collected from the shear zone for fabric analyses. Some samples are impregnated with epoxy and thin-sectioned for optical measurements of sand-particle fabrics. Sets of  $25\text{--}75$  samples ( $18\text{ mm}$  cubes) are also collected to measure anisotropy of magnetic susceptibility (AMS). These measurements yield orthogonal directions of maximum, intermediate and minimum magnetic susceptibility ( $k_1$ ,  $k_2$  and  $k_3$ , respectively) for each sample. Ancillary tests in which blocking temperatures and magnetic hysteresis (Tarling and Hrouda, 1993) are studied allow the source of the AMS to be determined (Hooyer and others, 2008). More details regarding the fabric analyses and procedure of these experiments can be found in Thomason and Iverson (2006), Hooyer and others (2008) and Iverson and others (2008).

Rather than reproducing data from these studies, herein we simply summarize the conclusions from this work that guide our field interpretations. Although numerical values differ slightly among different tills, the following generalizations apply to all of the tills that we have subjected to slow, simple shear:

AMS is due to the alignment of mostly silt-sized and smaller, non-equant magnetite grains present in small

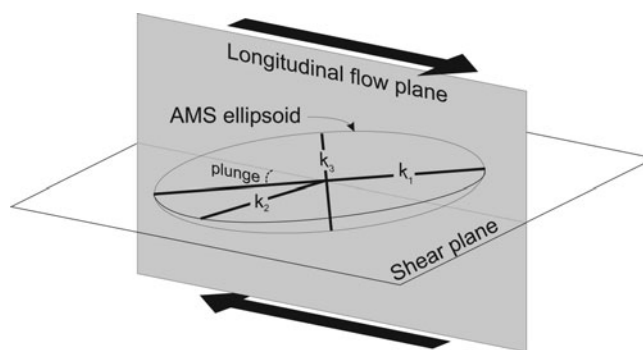


**Fig. 2.** Relationship between simple shear and directions of principal magnetic susceptibilities observed in ring-shear experiments that were carried out to strains greater than the critical value. The steady-state fabric formed by sand-grain long axes in experiments was similar to the  $k_1$  fabric (Thomason and Iverson, 2006).

quantities ( $<0.2\%$ ). The orientation of  $k_1$  reflects orientations of the long axes of these grains, with their magnetic signatures integrated over the volume of a sample ( $\sim 3.3\text{ cm}^3$ ).

Both sand-grain long axes and  $k_1$  orientations become tightly clustered in the direction of shear. These strong, steady-state fabrics are attained at moderate shear strains of  $7\text{--}30$ , with no evidence of systematic fabric weakening or strengthening with further strain. The shear strain above which fabric does not strengthen further is called the *critical strain* (Iverson and others, 2008). For the Batestown till, sand grains measured in the longitudinal flow plane yield a steady, two-dimensional,  $S_1$  eigenvalue, a measure of fabric strength (Mark, 1973), of  $0.74$ , with a standard error of  $0.032$ . Orientations of  $k_1$  yield steady three-dimensional  $S_1$  values of  $0.94$ , with a standard error of  $0.067$ .

Both sand-grain long axes and  $k_1$  orientations plunge up-glacier (Fig. 2). In the Batestown till, at strains sufficient for a steady fabric, sand grains plunge  $12^\circ$  and  $k_1$  orientations plunge  $28^\circ$ .

Both  $k_1$  and  $k_3$  lie in the longitudinal flow plane and therefore fully define its orientation. The orientation of  $k_2$  is normal to the longitudinal flow plane and thus lies within the plane of shear (Fig. 2).

Therefore, where tills have sand-particle and AMS fabric strengths less than steady-state ring-shear values, bearing in mind their uncertainty, a reasonable inference is that these tills have not been subjected to unidirectional simple shear to strains as high as  $7\text{--}30$ . In addition, fabrics will be oriented in the direction of shear. Moreover, for bed-parallel simple shear, fabrics should plunge up-glacier,  $k_1$  and  $k_3$  should both lie in a vertical flow plane, and  $k_2$  should be horizontal and oriented perpendicular to the shearing direction (Fig. 2).

We acknowledge that subglacial conditions are almost certainly more complex than those of our ring-shear experiments, but that is why the experiments are valuable: they show how fabric develops for the idealized case of bed-parallel simple shear. Isolating more complicated states of strain from till fabrics measured in the field seems unlikely without first understanding this simple case.

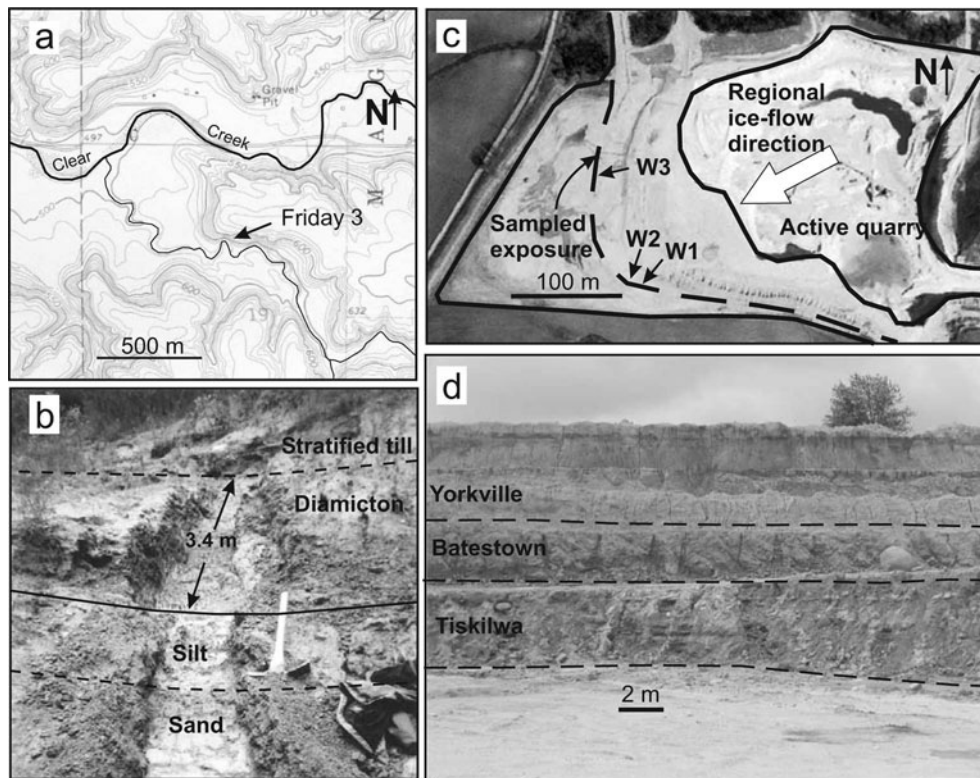


**Fig. 3.** (a) Topographic setting of the Friday 3 exposure. (b) Friday 3 exposure after trenching. (c) Oblique aerial view of the Wedron silica quarry and profiles W1–W3. (d) Wedron exposure of the Batestown Member and members deposited by earlier (Tiskilwa) and later (Yorkville) advances.

### 3. STUDY AREA AND GEOLOGICAL SETTING

Sediments associated with three major fluctuations of the Lake Michigan lobe during the late Wisconsin are regionally extensive in Illinois (Fig. 1) but are exposed only rarely, along stream cut-banks, within quarries and along road cuts. The second of these advances (17.7–18.5  $^{14}\text{C}$  ka BP) deposited the Batestown Member of the Lemont Formation (Hansel and Johnson, 1996). Two of this member's facies are massive-loam diamictons that are interpreted to be basal tills (Hansel and Johnson, 1996). This till can be up to 25 m thick in some end moraines, but pinches out beneath younger glacial deposits in northeast Illinois (Hansel and Johnson, 1996). Two sites were chosen for study where the Batestown Member is both exposed fully and easily accessible.

#### 3.1. Friday 3

Near Henry, Illinois, about 20 km up-glacier from the terminal margin of the Batestown advance, the Batestown Member and underlying deposits of the earlier Tiskilwa advance are exposed along a cut-bank of Clear Creek, a tributary to the Illinois River (Fig. 3a and b). This exposure was also described by Carlson and others (2004), who studied the Tiskilwa Member. Four glacial facies are associated with the Batestown advance at this site (Fig. 4a). Lowermost fluvial sands are overlain by lacustrine silts, both of which were presumably deposited proglacially. Overlying these sediments is a homogeneous loam diamicton (13% gravel, 59% sand, 28% silt/clay) that is about 3.6 m thick and has been interpreted to be a basal till in nearby outcrops (Johnson and Hansel, 1999). This till is overlain by thin beds of oxidized diamicton and sand and gravel, which are likely supraglacial, ice-marginal sediments.

#### 3.2. Wedron

At Wedron, Illinois, the Batestown Member is exposed in a large silica quarry, approximately 70 km up-glacier from the Batestown ice margin at its maximum extent (Fig. 3c and d). Johnson and Hansel (1990, 1999) described in this quarry four facies of the Batestown Member: a massive silty clay, two overlying mostly homogeneous diamictons and an uppermost layered diamicton containing sorted silts and sands (Fig. 4b). They interpreted these facies as deformed lake sediments, basal tills and a supraglacial till, respectively. The lake sediments contain occasional slickensides indicating deformation, and the overlying diamictons are compact, with moderately strong pebble fabrics ( $S_1 > 0.7$ ) in the direction of regional ice flow (60° southwest) and scattered deformed sand bodies.

The quarry sections studied by Johnson and Hansel (1990, 1999) are no longer accessible, but a different exposure in the quarry was located that differed only in that the uppermost facies consisted of bedded sand and gravel without diamicton. Our focus was the two basal till facies, which Johnson and Hansel (1990) first interpreted to be lodgment tills but later considered in the context of a deforming-bed model (Johnson and Hansel, 1999). The lower till is approximately 0.8 m thick and is fine-grained (8% gravel, 27% sand, 65% silt/clay) (Fig. 4b) with a moderately sharp to gradational contact with the underlying lake sediments. The protolith for this till may be lake sediments that were sheared subglacially (Johnson and Hansel, 1999). The upper contact of this facies with the overlying till facies is sharp. This overlying facies is coarser (15% gravel, 47% sand, 38% silt/clay) (Fig. 4b) and approximately 1.0 m thick.

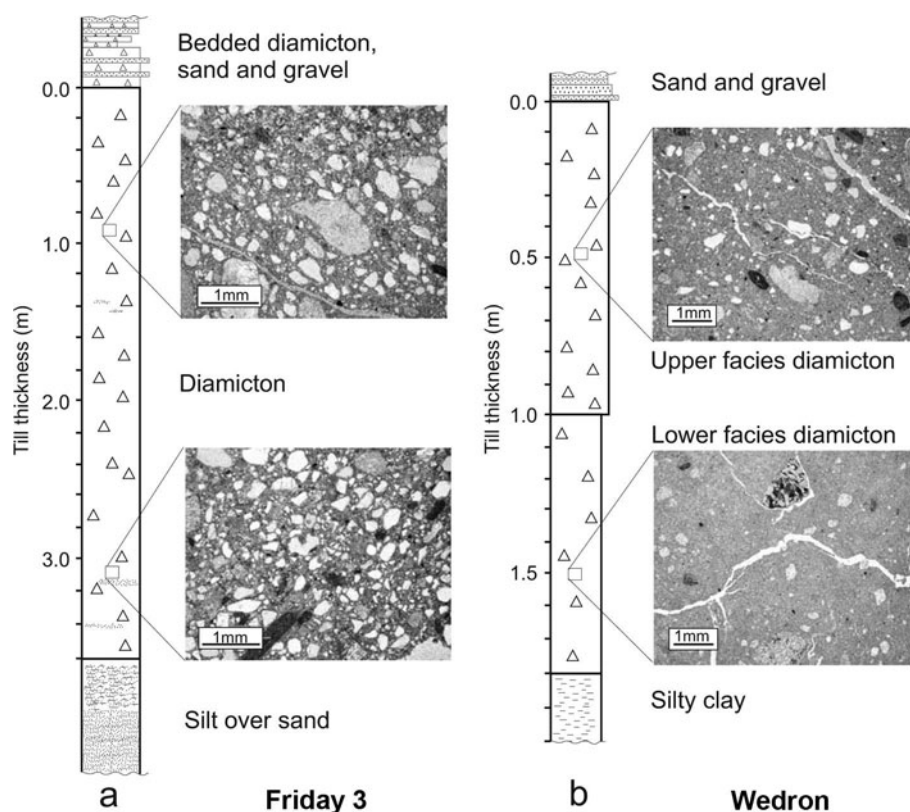


Fig. 4. Schematic stratigraphic columns at (a) Friday 3 and (b) Wedron. Photomicrographs show variability of till texture among sampling sites.

#### 4. FIELD SAMPLING

Intact samples of till were collected along profiles that extended over the full thickness of diamicton. AMS fabrics and sand-particle fabrics were measured along profiles at 0.2 m depth intervals. Measurements of bulk density (six to nine measurements) and pebble fabric (one measurement) were also made at each site.

Samples for AMS measurements were collected along a single profile at the Friday 3 site (Fig. 3b) and along three profiles at the Wedron site (W1–W3; Fig. 3d). W1 and W2 were 2 m apart; W3 was about 100 m from these profiles (Fig. 3c). At each sampling depth, till was excavated to expose a horizontal surface approximately 0.4 m long by 0.3 m wide. Excavation was extended sufficiently into the wall of the quarry to avoid modern pedogenic influence (~1.0 m at Friday 3; ~0.5 m at Wedron). A four-walled titanium box sampler was inserted downward into the till at the exposed surface, and its orientation was measured. The sampler was then excavated, and the encased till sample was carefully extruded into a plastic box of the same dimensions (18 mm × 18 mm × 18 mm) required for AMS measurements. This process was repeated until 25 samples were collected at the chosen depth. The principal susceptibilities,  $k_1$ ,  $k_2$  and  $k_3$ , were measured with a Geofyzika a.c. susceptibility KappaBridge located at the University of Minnesota Institute for Rock Magnetism. The familiar fabric analysis method of Mark (1973) was used to determine the fabric strengths defined by the alignment of  $k_1$  axes, as well as orientations of maximum clustering of  $k_1$ ,  $k_2$  and  $k_3$ . The  $k_1$  fabric strength was calculated as a normalized eigenvalue,  $S_1$ , which varies from 0.33 to 1.0 (uniform distribution of  $k_1$  orientations to perfect

alignment, respectively), for three-dimensional data.  $S_2$  and  $S_3$  values were also calculated from  $k_1$  orientations. The directions of the clustering of  $k_1$ ,  $k_2$  and  $k_3$  were described by their respective  $V_1$  eigenvectors, which are by definition, orthogonal.

In addition, intact samples of till were collected for sand-particle fabric analysis at Friday 3, W1 and W3 (Fig. 2). In some instances, a four-walled steel box sampler (30 mm × 30 mm × 50 mm in height) was tapped into an excavated till bench. However, in most cases a till block with dimensions similar to those of the sampler was excavated with a trowel and masonry hammer. The orientation of each block was measured upon excavation, and the blocks were then wrapped in plastic for transport to the laboratory. There they were dehydrated and impregnated with acetone and epoxy treatments, respectively (Clark, 1988). Following Evenson (1971), each epoxy-impregnated till block was thin-sectioned along two perpendicular planes to determine the azimuth (horizontal plane) and plunge (vertical plane) of elongate sand-sized particles. Between five and seven photomicrographs were taken of each 45 mm × 75 mm thin section, and the orientations of all sufficiently large and non-equant particles (long axes  $\geq 0.1$  mm and axial ratios  $\geq 1.5$ ) were measured. First, particles were measured in a horizontal plane, from which  $V_1$  was calculated. Then thin sections were made in a vertical plane parallel to  $V_1$ , and particle orientations were measured in that plane to compute  $S_1$ . This procedure was motivated by the observation that particles align parallel to the shearing direction (Hooyer and Iverson, 2000a), such that vertical thin sections parallel to  $V_1$  in a horizontal section would then be parallel to the local glacier-flow direction.

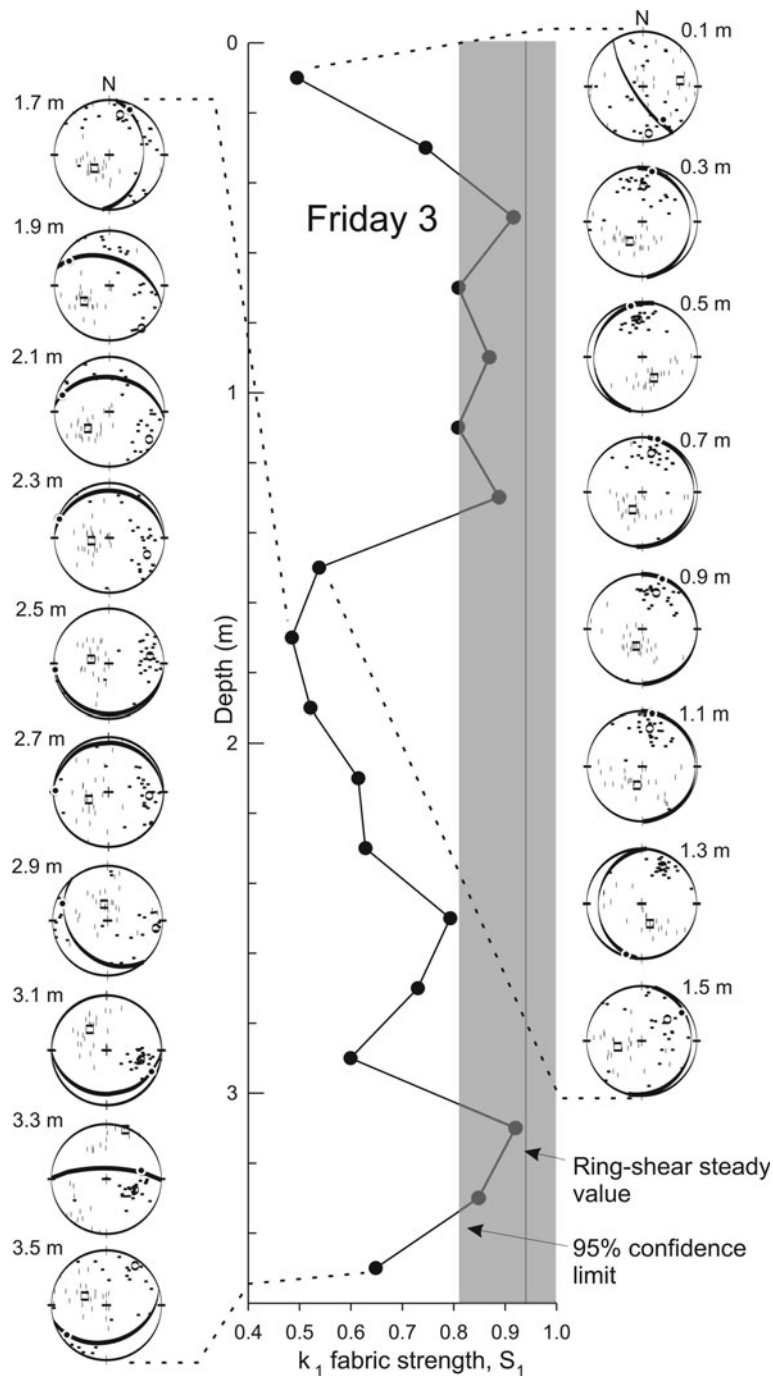


**Fig. 5.** AMS fabric strengths and directions as a function of depth at Friday 3. Horizontal and vertical marks in lower-hemisphere stereo plots are  $k_1$  and  $k_3$  orientations, respectively. Their respective eigenvectors ( $V_1$ ) are shown with open circles and squares. Great circles indicate planes of shear, as inferred by assuming only simple shear and directly applying relationships from ring-shear experiments (see text). Solid dots within those planes indicate the direction of shear.

## 5. RESULTS

### 5.1. Friday 3 $k_1$ and sand-grain fabrics

Laboratory experiments indicate that both  $k_1$  and sand-grain fabrics strengthen in the flow direction with shear deformation, so fabric strengths help indicate deformation magnitude. Figure 5 shows how  $k_1$  fabric strengths at Friday 3, as indicated by  $S_1$  values, vary with depth.  $S_1$  values are referenced to the steady-state, experimental fabric strength ( $S_1 = 0.94$ ) developed at moderate strains (7–30). Regression of the experimental data (Hooyer and others, 2008) allows a 95% lower confidence limit ( $S_1 = 0.81$ ) to be

specified for the steady-state experimental  $S_1$  value (Fig. 5).  $S_1$  values are larger than this lower limit near the top (0.5–1.3 m depth) and bottom (3.1–3.3 m) of the section. Over a broad range of depth in the middle (1.5–2.9 m) and at the very top (0.1–0.3 m) of the section, fabrics are weaker. The strongest fabrics measured have  $S_1$  values close to but not in excess of the steady-state ring-shear value. Depth variations in sand-grain fabric strength (Fig. 6) mimic variations in  $k_1$  fabrics to the extent that fabrics stronger than the 95% lower confidence limit occur near the top and bottom of the section. However, they occur over ranges of depth that are smaller than for the  $k_1$  fabrics (Fig. 6). The lower confidence

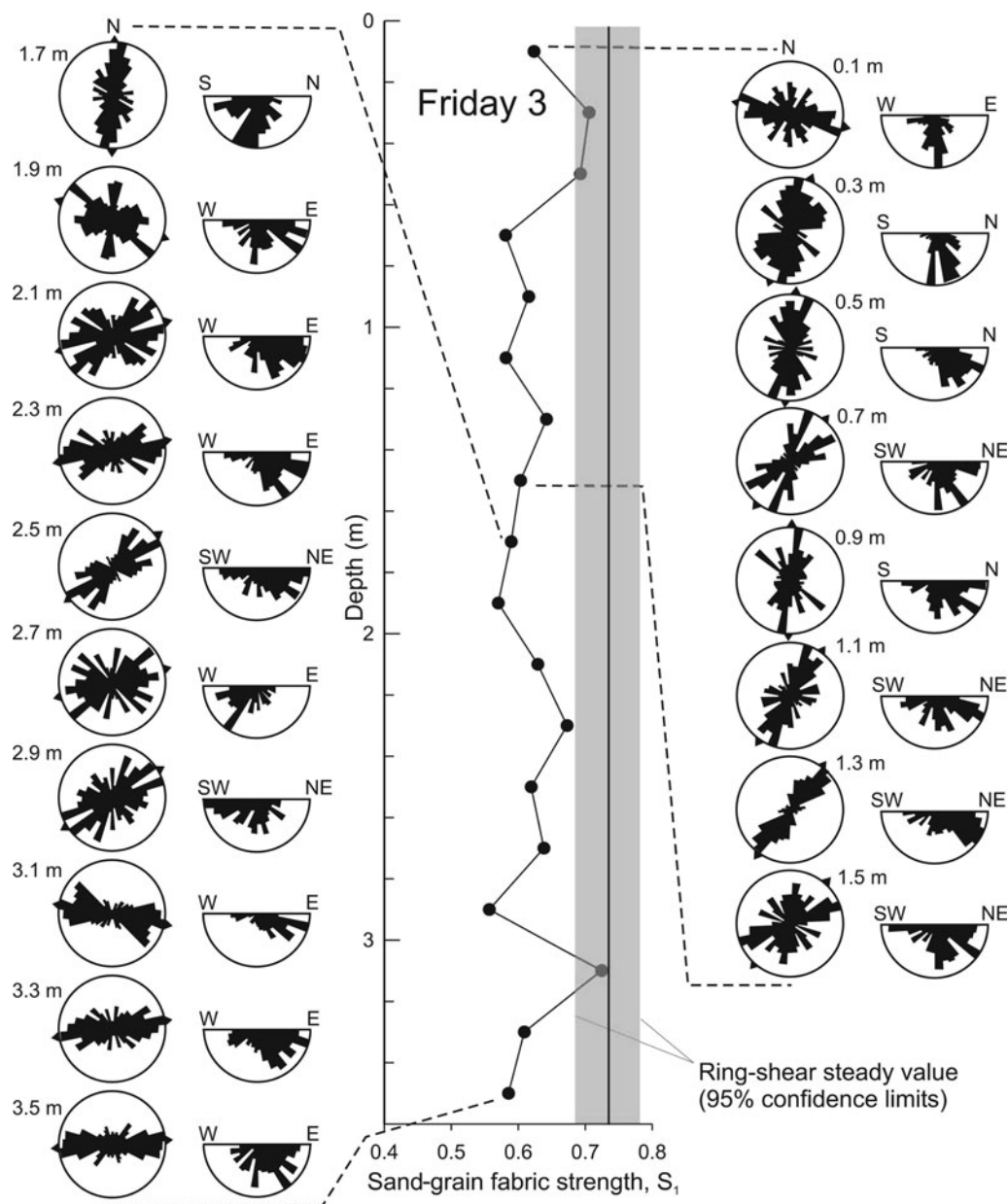


**Fig. 6.** Sand-grain long-axis fabric strength and direction as a function of depth at Friday 3. Full-circle diagrams display particle measurements in a horizontal plane. Triangular tick marks at circle perimeter indicate orientations of  $V_1$  (azimuths). Half-circle diagrams display particle measurements in a vertical plane parallel to  $V_1$ . Two-dimensional  $S_1$  values are based on orientations of particles in vertical thin sections, to allow direct comparison with measurements from ring-shear experiments.

limit in this case is calculated from regressions of ring-shear sand-grain data (Thomason and Iverson, 2006).

Fabric directions, which are described herein using the principal eigenvector  $V_1$  to characterize the direction of clustering, yield important information about strain orientation. Azimuths of  $k_1$  at Friday 3 vary from the bottom to the top of the section:  $k_1$  azimuths shift from  $\sim 90^\circ$  (east–west) to  $\sim 0^\circ$  (north–south) over the 3.5 m thickness of the section (Fig. 7a). Azimuths of sand-grain long-axis fabrics shift similarly (Fig. 7a). Plunges of  $k_1$  cluster around the steady value obtained in ring-shear experiments ( $28^\circ$  up-glacier) (Fig. 7b). The mean plunge at Friday 3 is  $23.5^\circ$  up-glacier (northeast), with a standard deviation of  $14.1^\circ$ . The mean plunge of the sand-grain long axes is similar but with more variability,  $25.1^\circ$  northeast  $\pm 34.4^\circ$  up-glacier (Fig. 7b). AMS measurements provide  $k_2$  values, which also reflect the state of strain. The mean plunge of  $k_2$  orientations is near zero

(mean =  $10.8^\circ$ ), but plunges change smoothly with depth and locally exceed  $40^\circ$  (Fig. 7c).

The relationship between the state of strain during simple shear and orientations of principal magnetic susceptibilities determined in ring-shear experiments provides a means of estimating the orientation of shear planes from AMS data. If simple shear is assumed, results from ring-shear experiments tell us that the plane of shear should be oriented normal to the longitudinal flow plane, as defined by  $k_1$  and  $k_3$  orientations. Also, this plane should be rotated  $\sim 28^\circ$  down-glacier around an axis defined by  $k_2$  orientations to account for the  $28^\circ$  up-glacier plunge of the  $k_1$  fabric. Stereonets of Figure 5 show the resultant shear-plane orientation implied by the AMS data from each depth, as well as the direction of shear within that plane. If simple shear dominated strain, then shear planes over some ranges of depth were close to horizontal (0.3–1.5 m, 2.3–2.7 m), but

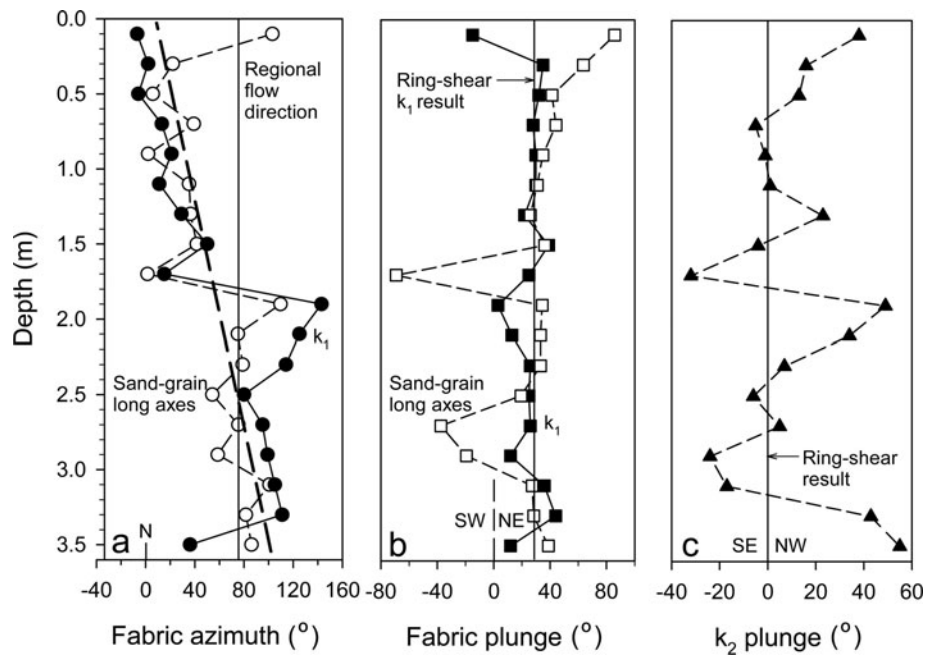


**Fig. 7.** (a) Azimuths ( $V_1$  orientations) of  $k_1$  and sand-grain fabrics at Friday 3. Dashed bold line is a regression of both the  $k_1$  and sand-grain data. The regional flow direction was estimated using the orientation of the terminal moraine of the Batestown advance, which is  $\sim 20$  km from the exposure. (b) Plunges of  $k_1$  and sand-grain fabrics. Ring-shear results for  $k_1$  are shown; sand grains plunged  $12^\circ$  up-glacier in ring-shear tests. (c) Plunge of  $k_2$  compared with the result from ring-shear tests.

elsewhere they were commonly inclined more than  $20^\circ$ . Dip directions of these shear planes are locally at a high angle ( $>45^\circ$ ) to the inferred shear direction (e.g. at depth 1.7 m).

### 5.2. Wedron $k_1$ and sand-grain fabrics

Depth-averaged  $k_1$  and sand-grain fabrics at Wedron are generally stronger than those at Friday 3 (Figs 8 and 9). The lowermost 70% of profiles W1 and W2 (0.5–1.7 m), which were only 2 m apart, have  $k_1$  fabric strengths with  $S_1$  values in excess of the lower 95% confidence limit for till sheared to moderate strains (7–39) (Fig. 8). There is no abrupt change in fabric strength across the facies contact at  $\sim 1.0$  m, but the fabric weakens notably over the uppermost 0.5 m of the section. Depth variation of the strengths of sand-grain fabrics collected at W1 is somewhat similar: low in the section,  $S_1$  values exceed the lower 95% confidence limit, although in this case these strong fabrics are restricted to the upper three-quarters of the lower facies (Fig. 9). At profile W3, which was  $\sim 100$  m from W1 and W2,  $k_1$  fabrics are somewhat weaker in the lowermost three-quarters of the section (Fig. 9) than at W1 and W2. Sand-grain fabrics are uniformly weak:  $S_1$  values nowhere exceed the lower 95% confidence limit. As at Friday 3, the largest  $S_1$  values for both  $k_1$  and sand-grain fabrics are close to or equal to the steady-state ring-shear value but do not exceed it.

Similar to Friday 3, azimuths of  $k_1$  fabrics at the three profiles display systematic depth variation (Fig. 10a). Although there is considerable variability among the profiles, moving up-section, the profile-averaged azimuthal variation is from  $\sim 40^\circ$  (northeast–southwest) to  $\sim 90^\circ$  (east–west). Azimuths of the sand-grain fabrics indicate a similar up-section variation in azimuth (Fig. 10b). This variation in fabric direction has the opposite sign to the variation observed up-section at Friday 3, where azimuths rotate up-section from approximately east–west to north–south.

Although at Wedron fabric strengths and azimuths do not change abruptly across the contact between the two till facies, fabric plunges do (Fig. 10c). Within the lower till facies,  $k_1$  fabrics generally plunge up-glacier, consistent with results from Friday 3. However, in the upper till facies,  $k_1$  fabrics plunge uniformly down-glacier at an average of  $21^\circ$ . Sand grains indicate a similar change in fabric plunge, although the change to down-glacier plunging fabrics occurs high within the upper facies, rather than across the contact with the upper facies (Fig. 10d). As at Friday 3, plunges of  $k_2$  cluster around 0 (mean =  $1.0^\circ$ ), vary with depth and at some depths are large (Fig. 10e);  $k_2$  plunges do not vary systematically across the facies contact.

If, as at Friday 3, we use directions of principal magnetic susceptibility to determine the orientation of shear planes, assuming that simple shear dominated strain, then most of the inferred shear planes, unlike at Friday 3, dip at angles in excess of  $20^\circ$  (Fig. 8). Many of the largest dips ( $>40^\circ$ ) are in the down-glacier direction and in the upper till facies: a result of the down-glacier  $k_1$  plunges in that facies (Fig. 10c).

### 5.3. Fabric shape

Thus far, in discussing fabric strengths, we have considered only  $S_1$  values, but there can be additional information contained in  $S_2$  and  $S_3$  values (e.g. Benn, 1994; Bennett and others, 1999). Our focus here is the AMS data, since they are fully three-dimensional (there would be no point in studying  $S_2$  variation for the two-dimensional sand-grain data because in that case,  $S_1 = 1 - S_2$ ). If  $S_1$  values based on  $k_1$  orientations for all depths at both Friday 3 and Wedron are plotted against  $S_3$  values for these orientations, 49% of the values plot within the 95% confidence limit for fabrics attained at strains that exceed the critical value (7–30) (Fig. 11a). This confidence limit was determined from ring-shear data in which  $S_1$  and  $S_3$  values were regressed against known strain magnitudes. The

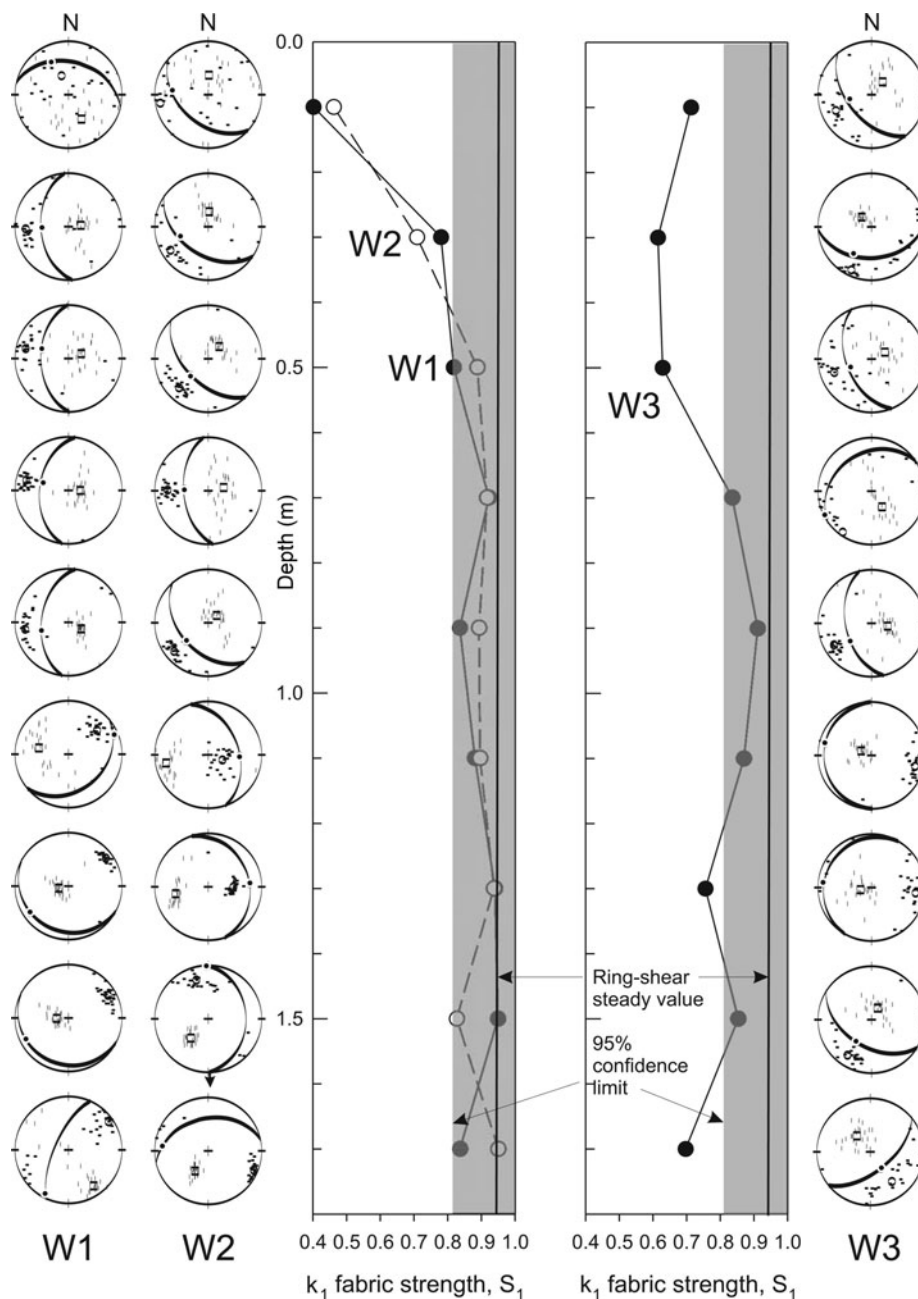


**Fig. 8.** AMS fabric strengths and directions as a function of depth at W1–W3. Horizontal and vertical marks in lower-hemisphere stereo plots are  $k_1$  and  $k_3$  orientations, respectively. Their respective eigenvectors ( $V_1$ ) are shown with open circles and squares. Great circles indicate planes of shear, as inferred by assuming only simple shear and directly applying relationships from ring-shear experiments (see text). Solid dots within those planes indicate the direction of shear. W1 and W2 were about 2 m apart; W3 was ~100 m away.

ternary diagrams of Benn (1994) provide additional insight into fabric strengths by including all of the principal eigenvalues. Again, 49% of the data fall within the 95% confidence interval for fabric shapes attained at strains that exceed the critical value (Fig. 11b).

**5.4. Comparison of directions of  $k_1$  and sand-grain fabrics**

Comparison of directions of  $k_1$  and sand-grain fabrics indicates that these two methods of fabric characterization yield results that are correlated but with significant variability (Fig. 12a and b). The average angular distance along great circles between  $k_1$  and sand-grain principal eigenvectors is  $36.6^\circ$ , with a standard deviation of  $26.8^\circ$ .

**5.5. Bulk densities and pebble fabric**

At Wedron there is a clear difference in bulk density between the lower till facies ( $2.0 \pm 0.06 \text{ g cm}^{-3}$ ) and upper till facies ( $2.3 \pm 0.05 \text{ g cm}^{-3}$ ). Bulk-density values at Friday 3 are the same as those of upper facies at Wedron ( $2.3 \pm 0.04 \text{ g cm}^{-3}$ ) and relatively uniform throughout the section (Thomason, 2006, p.136). Pebble fabrics, measured over very broad areas ( $\sim 40 \text{ m}^2$ ) owing to the sparseness of pebbles, plunged to the northeast at both locations ( $22^\circ$ ) and were weaker ( $S_1 = 0.60$  at Wedron;  $S_1 = 0.55$  at Friday 3) than pebble fabrics reported at Wedron by Johnson and Hansel (1990) ( $S_1 \sim 0.7$ ).

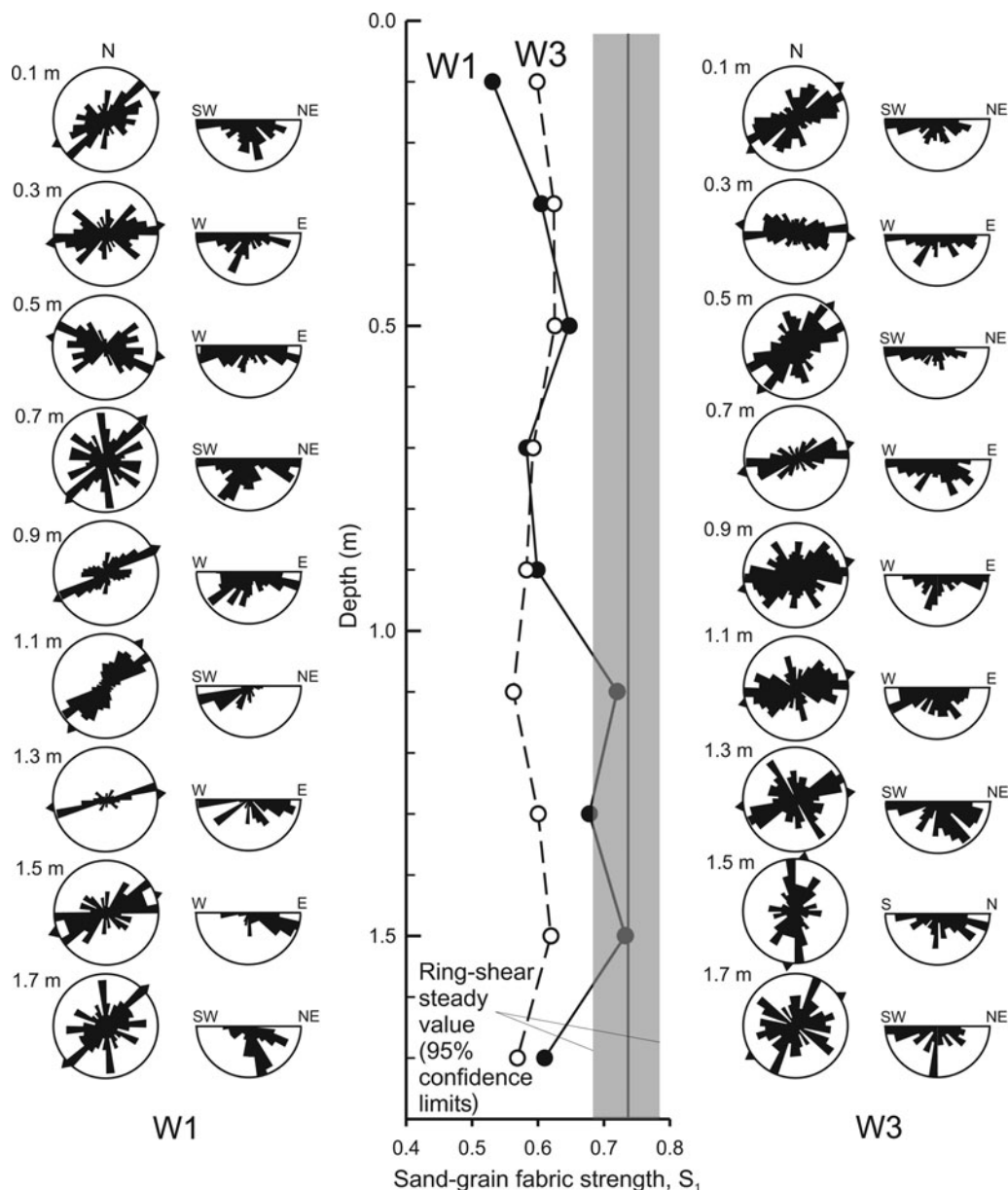


**Fig. 9.** Sand-grain long-axis fabric strength and direction as a function of depth at W1 and W3. Full-circle diagrams display particle measurements in a horizontal plane. Triangular tick marks at circle perimeter indicate orientations of  $V_1$  (azimuths). Half-circle diagrams display particle measurements in a vertical plane parallel to  $V_1$ . Two-dimensional  $S_1$  values are based on orientations of particles in vertical thin sections, to allow direct comparison with measurements from ring-shear experiments.

## 6. DISCUSSION

### 6.1. Fabric strength and direction

Large, relatively smooth depth variations of  $S_1$  values from  $k_1$  and sand-grain fabrics indicate that strain magnitude in the Batestown till was insufficient over some depth ranges to be consistent with the bed-deformation model (Figs 5, 6, 8 and 9). Fabric-strength indicators that are less than the lower 95% confidence limits of Figures 5, 6, 8, 9 and 11 indicate a less than 5% chance that these till samples were sheared to the critical shear strain (7–30). Thus, 25–100% of a given profile and 51% of the total number of till samples have fabrics too weak to reflect shear to even moderate strains. These conclusions are essentially the same, regardless of whether we consider AMS fabric strength based only on  $S_1$  eigenvalues (Figs 5 and 8) or on fabric indicators that involve the other eigenvalues (Fig. 11).

Significant zones in the till, however, do have fabrics sufficiently strong to be consistent with strains greater than or equal to the critical value. For example,  $k_1$  fabric strengths from 0.5 to 1.3 m at Friday 3 (Fig. 5) and the lowest 75% of the two facies at Wedron (Fig. 8) indicate that such strains could have been attained or exceeded. With the exception of profile W3, sand fabrics also point to such strain magnitudes, although over more limited ranges of depth (Figs 6 and 9). The observation that in six of the seven fabric profiles of Figures 5, 6, 8 and 9,  $S_1$  values approach closely but do not exceed the steady-state  $k_1$  and sand-grain  $S_1$  values from ring-shear experiments indicates that the experiments seem to have accurately predicted the maximum fabric strengths that were developed subglacially.

Nevertheless, in inferring strain magnitude from these data, several caveats apply. Fabrics necessarily provide

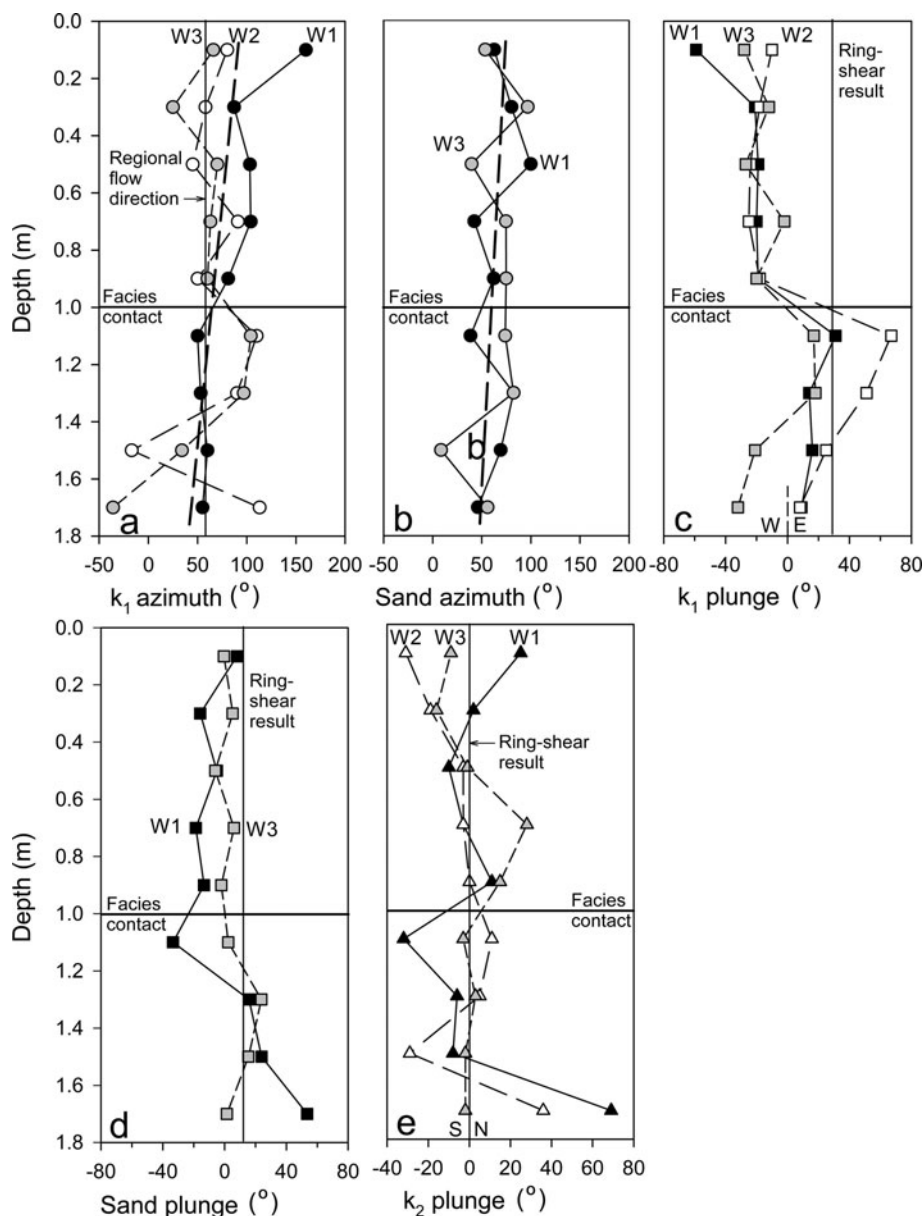


**Fig. 10.** (a) Azimuths ( $V_1$  orientations) of  $k_1$  fabrics at W1–W3. Dashed bold line is a regression of the data. The regional flow direction was assumed to be the clast-fabric direction measured by Hansel and Johnson (1996). (b) Azimuths of sand-grain fabrics at W1 and W3. (c) Plunges of  $k_1$  fabrics at W1–W3 and ring-shear result. (d) Plunges of sand-grain fabrics at W1 and W3 with ring-shear result. (e) Plunges of  $k_2$  at W1–W3 compared with the result from ring-shear tests.

information about only the most recent deformation to have set the fabric. Similarly, although we have no evidence for post-shear disturbance of fabric, we cannot preclude it. Most importantly, the strong fabrics that fall within the confidence limits for till sheared to the critical strain do not strictly demonstrate that such strains occurred. For example, if fabric was partly inherited from oriented particles in basal ice upon lodgment, then the critical strain required to reach the steady-state fabric strength would have been smaller than in the experiments. Moreover, the critical strain determined in ring-shear experiments (7–30) is less than that required by the bed-deformation model (>100). Thus, in the absence of post-shear disturbance, weak fabrics rule out the high strains of the bed-deformation model, but strong fabrics do not demonstrate that such strains were attained (Thomason and Iverson, 2006; Hooyer and others, 2008; Iverson and others, 2008).

Both  $k_1$  and sand-grain fabrics indicate that shearing direction changed systematically up-section within the till: from approximately east–west to north–south at Friday 3 (Fig. 7a) and in the reverse direction at Wedron (Fig. 10a and b). This observation is not consistent with the till layer shearing simultaneously over its full thickness. Carlson and others (2004) reached a similar conclusion for the underlying Tiskilwa till based on depth variation of pebble fabric azimuths, although depth resolution of that study was limited to 1.0 m. The depth scale of fabric azimuthal variation in our study indicates simultaneous deformation over thicknesses of no more than a few decimeters.

Shear-plane orientations inferred from directions of principal susceptibilities at Friday 3 indicate some depth ranges where shear planes were essentially horizontal (0.3–1.5 m, 2.3–2.7 m) and hence consistent with bed-parallel simple shear (Fig. 5). These depth ranges correspond

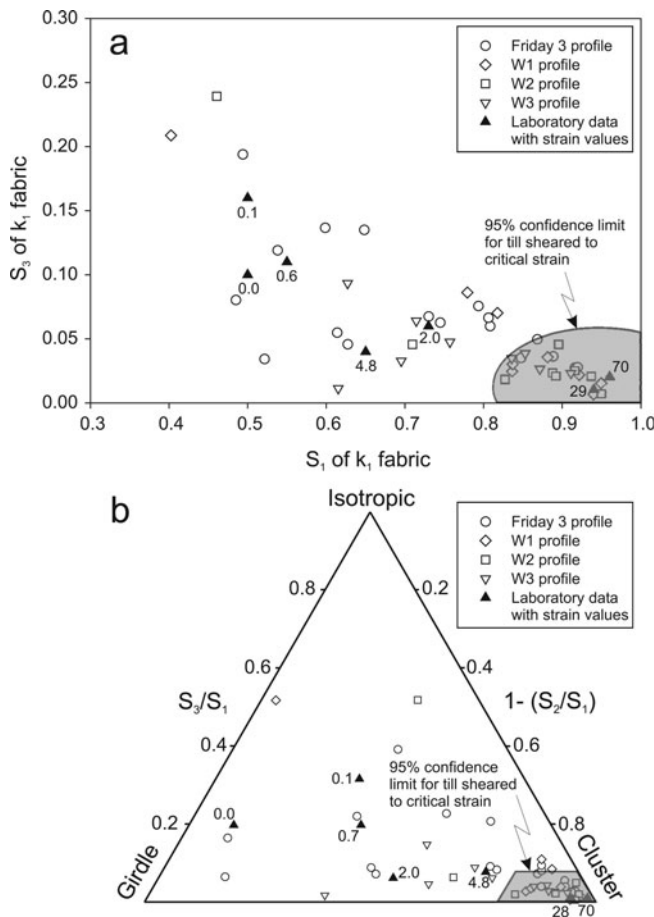


**Fig. 11.** (a) Bivariate and (b) Benn (1994)-style plots based on  $k_1$  orientations. Numbers next to experimental values indicate the strain at which the fabric was measured. Till with fabric strengths that plot outside the shaded regions has less than a 5% chance of having been sheared to the critical strain.

to those where both  $k_1$  and  $k_2$  plunges are close to those expected from ring-shear tests (Fig. 7b and c). Cluster of  $k_1$  and  $k_2$  plunges about means that agree with the results of the ring-shear tests suggests again that the experiments provide a valid basis for field interpretations.

Deviation of  $k_1$  and  $k_2$  plunges from ring-shear values over other depth ranges at Friday 3 (Fig. 7b and c) and more conspicuously at Wedron (Fig. 10c–e) must reflect deviations from bed-parallel simple shear. These deviations could be interpreted, as expressed in the stereonets of Figures 5 and 8, as simple shear inclined to the horizontal, or as significant components of pure shear superimposed on bed-parallel simple shear. A well-established precept of structural geology is that any state of strain can result either from pure shear or from simple shear inclined at an appropriate angle (Hobbs and others, 1976, p. 32). Thus, for example,  $k_2$  plunges in Figure 7c that deviate significantly from zero can be interpreted either as shear that occurred in a plane with a large transverse dip component or as bed-parallel simple shear with transverse shortening superimposed on that shear. More enigmatically, at Wedron there is an abrupt shift in  $k_1$  plunge from largely up-glacier (east) in the lower till facies to uniformly down-glacier (west) in the upper till facies (Fig. 10c and d). Inferred shear planes in the upper facies, therefore, tend to dip steeply down-glacier. This could reflect a major deviation from simple shear, associated perhaps with longitudinal shortening or till accretion from

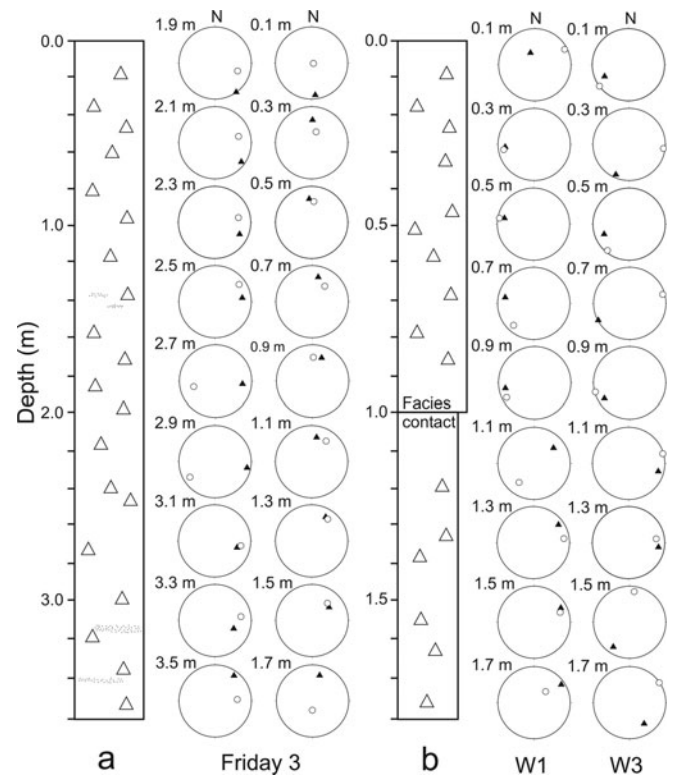


**Fig. 12.** Fabrics directions ( $V_1$ ) based on  $k_1$  orientations (black triangles) and sand-grain orientations (circles) on lower-hemisphere stereo plots. Sand-grain data reflect measurements in horizontal and vertical thin sections as described in the text.

basal ice on a paleoslope inclined down-glacier (personal communication from D. Evans, 2008).

An ancillary objective of this study was to compare  $k_1$  fabrics with sand-grain fabrics. There is considerable correspondence between  $k_1$  and sand-grain fabric azimuths (Fig. 12), in agreement with the experimental finding that  $k_1$  fabrics align in the direction of the long axes of particles (Hooyer and others, 2008). However, the correspondence is far from perfect. We do not know the reason for this difference in  $k_1$  and sand-grain fabric orientations but suspect that it is due primarily to some combination of the measurement uncertainty, inherent variability, and two-dimensionality of sand-grain fabrics. Optical measurement of sand-grain long axes in thin sections involves human error and subjectivity that is largely absent in the measurement of AMS principal susceptibilities (Iverson and others, 2008). In addition, sand-grain fabric signals will be inherently more variable than  $k_1$  signals because a single  $k_1$  measurement reflects the volume integration of the effects of many aligned magnetic grains in a sample, rather than the orientation of a single grain (Hooyer and others, 2008). Also, additional uncertainty is introduced by the difference between true sand-grain orientations and apparent orientations measured in thin sections.

## 6.2. Interpretation of till deformation

These fabric measurements leave little doubt that the Batestown till was deformed (e.g. Johnson and Hansel, 1999), but the picture that emerges is that this deformation commonly deviated from the high strains required of the bed-deformation model and the deep, simple shear of the bed that is frequently assumed. The up-section shift in fabric azimuth at both locations (Figs 7b and 10a and b) indicates that the full till thickness did not shear simultaneously. Rather, till

likely sheared in a layer a few decimeters thick near the glacier sole, as till progressively accreted to the bed from ice and the shear direction in the till changed with time. Variability in fabric strength with depth (Figs 5, 6, 8 and 9) therefore suggests temporal variability in the magnitude of bed deformation near the glacier sole: strain during some periods equaled or exceeded the critical strain required for steady-state fabric development and during other periods fell short of the critical strain. In addition, bed-parallel simple shear of the bed did not occur over many depth ranges, as indicated by inferred shear planes that dip substantially (Figs 5 and 8). This implies either that shear planes were indeed inclined or that there were significant components of pure shear. In either case, there were apparently three-dimensional effects that locally caused major deviations from simple shear. This inferred state of strain is consistent with till deformation focused in three-dimensional patches (e.g. Piotrowski and Kraus, 1997), either causing shear zones to dip near the margins of patches or alternatively causing significant local shortening or extension of the till layer.

What caused shear direction to change with time? Two timescales of variation are evident: the secular azimuthal variation across the till thickness as indicated by the slopes of the regression lines in Figures 7a and 10a and b, and the higher-frequency azimuthal variability about the regression lines over depth ranges of decimeters. The secular azimuthal shift likely reflects how flow direction changed as the Lake Michigan lobe retreated. Moraine geometry, which indicates the lobe broke into smaller sub-lobes during retreat, provides support for this hypothesis at Friday 3 (Fig. 13a–c). The terminal moraine of the Batestown advance, the Eureka moraine, is oriented north–south, consistent with ice flow from the east during the Batestown maximum and the associated east–west-trending fabric near the base of the Friday 3 section (Fig. 7a). Inboard of the Eureka moraine and within 10 km of Friday 3, the recessional Arispie moraine is oriented east–southeast, consistent with the north–northeast fabric azimuth near the top of the section (Fig. 7a). Near Wedron, on the other hand, recessional moraines are oriented closer to north–south, such that, during glacier retreat in that area, flow would have been from approximately the east, consistent with fabric azimuth near the top of the Wedron section (Fig. 10a and b). The up-section northeast-to-east rotation of the fabric at Wedron could thus be explained if prior to retreat in this area flow was dominantly from the northeast, as seems likely given the general southwest flow of the lobe out of the Lake Michigan basin (Fig. 1). The higher-frequency azimuthal variations superimposed on the secular shifts are consistent with heterogeneous shallow deformation: temporally variable, patchy deformation of the bed would have resulted in zones of till convergence and divergence and associated shifts in shear direction as till accumulated and the geometry of deforming patches changed. Some of this high-frequency variability may be random noise (e.g. Benn and Ringrose, 2001), but some is not. For example, from 1.7 to 2.6 m depth at Friday 3, variability about the secular shift in azimuth is nearly identical for both  $k_1$  and sand-grain azimuths (Fig. 7a).

This picture of shallow heterogeneous deformation during till accretion from basal ice agrees with the interpretations of Piotrowski and colleagues based on diverse field observations of basal tills of the Fennoscandian ice sheet (Piotrowski and Kraus, 1997; Larsen and Piotrowski, 2003; Larsen and others, 2004, 2007; Piotrowski and others,

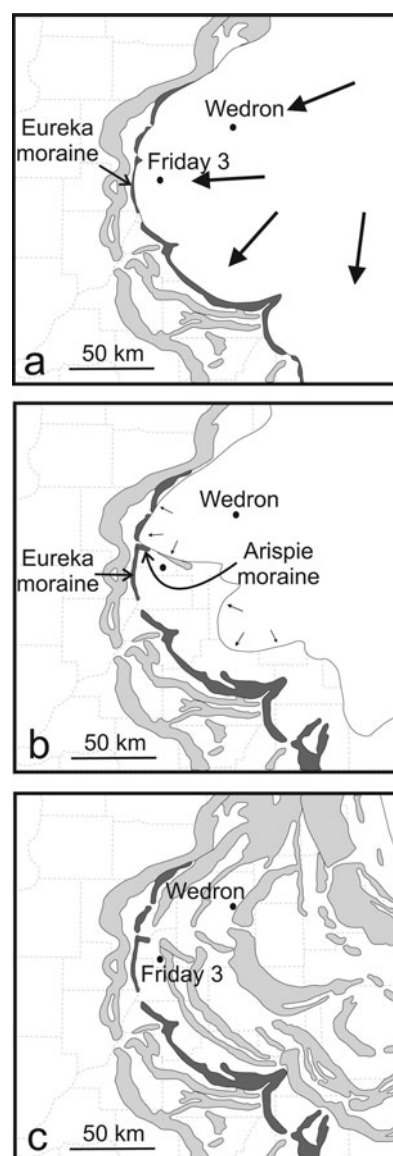


**Fig. 13.** (a) Maximum extent of the Lake Michigan lobe during the Batestown advance. (b) Possible configuration of the lobe during its retreat from the Eureka end moraine. (c) Final moraine configuration of the lobe. End moraine of the Batestown advance is indicated by dark gray. All other Wisconsin episode moraines are light gray.

2004). Heterogeneous, temporally variable bed deformation was also stressed by Evans and others (2006) in their review of basal till characteristics and genesis. This interpretation is also supported by measurements beneath modern soft-bedded ice masses. These measurements indicate that steep spatial gradients in water pressure at the bed are common (e.g. Murray and Clarke, 1995; Engelhardt and Kamb, 1997; Fischer and Clarke, 2001), and measurements of till deformation and sliding indicate that basal water pressure modulates the extent of bed deformation (Blake and others, 1994; Iverson and others, 1995, 1999, 2003, 2007; Fischer and Clarke, 1997, 2001; Fischer and others, 1999; Boulton and others, 2001) by regulating both till shear strength and the coupling between till and the glacier sole. Thus, heterogeneous deformation of the bed, with only patches of the bed deforming, is expected (e.g. Fischer and Clarke, 2001) and is indeed more consistent with subglacial measurements than the spatially pervasive simple shear of the bed that has often been assumed.

## 7. CONCLUSIONS

The Batestown advance of the Lake Michigan lobe resulted in deformation of its basal till, but deformation was different from that of many applications of the bed-deformation model:

At least half of the till studied was not sheared to even moderate strains (7–30).

Depths of bed deformation did not exceed a few decimeters.

Shearing was accompanied by progressive till accretion to the bed from ice, such that sediment transport by ice was important.

Till deformation commonly deviated from bed-parallel simple shear, indicating that deformation was not only shallow but spatially heterogeneous.

Although these conclusions do not preclude bed deformation as a contributor to the flow or landform development of the lobe, they suggest that deep, spatially pervasive, simple shear of the bed to high strains is likely a poor idealization in assessing the flow dynamics and sediment transport of the lobe.

## ACKNOWLEDGEMENTS

We thank N. Vreeland, who provided energetic assistance in the field, and M. Jackson and the University of Minnesota Institute for Rock Magnetism for making the AMS measurements possible. We also thank A. Hansel (Illinois State Geological Survey, Emeritus) for directing us to field sites, and D. Evans and an anonymous reviewer for helpful criticism. This work was supported by a grant from the US National Science Foundation (EAR-0444921).

## REFERENCES

- Alley, R.B. 1991. Deforming-bed origin for southern Laurentide till sheets? *J. Glaciol.*, **37**(125), 67–76.
- Alley, R.B., D.D. Blankenship, C.R. Bentley and S.T. Rooney. 1987. Till beneath Ice Stream B. 3. Till deformation: evidence and implications. *J. Geophys. Res.*, **92**(B9), 8921–8929.
- Anandakrishnan, S., G.A. Catania, R.B. Alley and H.J. Horgan. 2007. Discovery of till deposition at the grounding line of Whillans Ice Stream. *Science*, **315**(5820), 1835–1838.
- Baligh, M.M. 1972. Applications of plasticity theory to selected problems in soil mechanics. (PhD thesis, California Institute of Technology.)
- Baligh, M.M. 1985. Strain path method. *J. Geotech. Eng.*, **111**(9), 1108–1136.
- Benn, D.I. 1994. Fabric shape and the interpretation of sedimentary fabric data. *J. Sediment. Res.*, **A64**(4), 910–915.
- Benn, D.I. 1995. Fabric signature of subglacial till deformation, Breiðamerkurjökull, Iceland. *Sedimentology*, **42**(5), 735–747.
- Benn, D.I. 2002. Discussion and reply: clast-fabric development in a shearing granular material: implications for subglacial till and fault gouge. *Geol. Soc. Am. Bull.*, **114**(3), 382.
- Benn, D.I. and D.J.A. Evans. 1996. The interpretation and classification of subglacially-deformed materials. *Quat. Sci. Rev.*, **15**(1), 23–52.
- Benn, D.I. and T.J. Ringrose. 2001. Random variation of fabric eigenvalues: implications for the use of a-axis fabric data to differentiate till facies. *Earth Surf. Process. Landf.*, **26**(3), 295–306.
- Bennett, M.R., R.I. Waller, N.F. Glasser, M.J. Hambrey and D. Huddart. 1999. Glacigenic clast fabrics: genetic fingerprint or wishful thinking? *J. Quat. Sci.*, **14**(2), 125–135.
- Blake, E.W., U.H. Fischer and G.K.C. Clarke. 1994. Direct measurement of sliding at the glacier bed. *J. Glaciol.*, **40**(136), 595–599.
- Boulton, G.S. 1976. The origin of glacially fluted surfaces: observations and theory. *J. Glaciol.*, **17**(76), 287–309.
- Boulton, G.S. 1987. A theory of drumlin formation by subglacial sediment deformation. In Menzies, J. and J. Rose, eds. *Drumlin symposium: Proceedings of the Drumlin Symposium, First International Conference on Geomorphology, Manchester, 16–18 September 1985*. Rotterdam, A.A. Balkema, 25–80.
- Boulton, G.S. 1996a. The origin of till sequences by subglacial sediment deformation beneath mid-latitude ice sheets. *Ann. Glaciol.*, **22**, 75–84.
- Boulton, G.S. 1996b. Theory of glacial erosion, transport and deposition as a consequence of subglacial sediment deformation. *J. Glaciol.*, **42**(140), 43–62.
- Boulton, G.S., K.E. Dobbie and S. Zatsepin. 2001. Sediment deformation beneath glaciers and its coupling to the subglacial hydraulic system. *Quat. Int.*, **86**(1), 3–28.
- Carlson, A.E., J.W. Jenson and P.U. Clark. 2004. Sedimentological observations from the Tiskilwa Till, Illinois, and Sky Pilot Till, Manitoba. *Géogr. Phys. Quat.*, **58**(2–3), 229–239.
- Carr, S.J. and J. Rose. 2003. Till fabric patterns and significance: particle response to subglacial stress. *Quat. Sci. Rev.*, **22**(14), 1415–1426.
- Cladouhos, T.T. 1999. Shape preferred orientations of survivor grains in fault gouge. *J. Struct. Geol.*, **21**(4), 419–436.
- Clark, J.S. 1988. Stratigraphic charcoal analysis on petrographic thin sections: application to fire history in northwestern Minnesota. *Quat. Res.*, **30**(1), 81–91.
- Clark, P.U. 1991. Striated clast pavements: products of deforming subglacial sediment? *Geology*, **19**(5), 530–533.
- Clark, P.U. 1994. Unstable behavior of the Laurentide ice sheet over deforming sediment and its implications for climate change. *Quat. Res.*, **41**(1), 19–25.
- Clark, P.U. 1997. Sediment deformation beneath the Laurentide ice sheet. In Martini, I.P., ed. *Late glacial and postglacial environmental changes: Quaternary, Carboniferous–Permian and Proterozoic*. New York, Oxford University Press, 81–97.
- Clark, P.U. and D. Pollard. 1998. Origin of the middle Pleistocene transition by ice sheet erosion of regolith. *Paleoceanography*, **13**(1), 1–9.
- Clark, P.U., R.B. Alley and D. Pollard. 1999. Northern Hemisphere ice-sheet influences on global climate change. *Science*, **286**(5442), 1104–1111.
- Clayton, L., D.M. Mickelson and J.W. Attig. 1989. Evidence against pervasively deformed bed material beneath rapidly moving lobes of the southern Laurentide ice sheet. *Sediment. Geol.*, **62**(3–4), 203–208.
- Dowdeswell, J.A. and M.J. Siegert. 1999. Ice-sheet numerical modelling and marine geophysical measurements of glacier-derived sedimentation on the Eurasian Arctic continental margins. *Geol. Soc. Am. Bull.*, **111**(2), 1080–1097.
- Dowdeswell, J.A., M.J. Hambrey and R. Wu. 1985. A comparison of clast fabric and shape in Late Precambrian and modern glacigenic sediments. *J. Sediment. Petrol.*, **55**(5), 691–704.
- Drake, L.D. 1977. Human factor in till-fabric analysis. *Geology*, **5**(3), 180–184.
- Engelhardt, H. and B. Kamb. 1997. Basal hydraulic system of a West Antarctic ice stream: constraints from borehole observations. *J. Glaciol.*, **43**(144), 207–230.
- Evans, D.J.A., E.R. Phillips, J.F. Hiemstra and C.A. Auton. 2006. Subglacial till: formation, sedimentary characteristics and classification. *Earth-Sci. Rev.*, **78**(1–2), 115–176.
- Evenson, E.B. 1971. The relationship of macro- and microfabric of till and the genesis of glacial landforms in Jefferson County,

- Wisconsin. In Goldthwait, R.P., ed. *Till: a symposium*. Columbus, OH, Ohio State University Press, 345–364.
- Eyles, N., T.E. Day and A. Gavican. 1987. Depositional controls on the magnetic characteristics of lodgement tills and other glacial diamict facies. *Can. J. Earth Sci.*, **24**(12), 2436–2458.
- Fischer, U.H. and G.K.C. Clarke. 1997. Stick-slip sliding behaviour at the base of a glacier. *Ann. Glaciol.*, **24**, 390–396.
- Fischer, U.H. and G.K.C. Clarke. 2001. Review of subglacial hydro-mechanical coupling: Trapridge Glacier, Yukon Territory, Canada. *Quat. Int.*, **86**(1), 29–43.
- Fischer, U.H., G.K.C. Clarke and H. Blatter. 1999. Evidence for temporally varying “sticky spots” at the base of Trapridge Glacier, Yukon Territory, Canada. *J. Glaciol.*, **45**(150), 352–360.
- Fuller, M.D. 1962. A magnetic fabric in till. *Geol. Mag.*, **99**(3), 233–237.
- Gravenor, C.P. and M. Stupavsky. 1975. Convention for reporting magnetic anisotropy of till. *Can. J. Earth Sci.*, **12**(6), 1063–1069.
- Gravenor, C.P., M. Stupavsky and D.T.A. Symons. 1973. Paleomagnetism and its relationship to till deposition. *Can. J. Earth Sci.*, **10**(7), 1068–1078.
- Hansel, A.K. and W.H. Johnson. 1996. Wedron and Mason groups: lithostratigraphic reclassification of deposits of the Wisconsin Episode, Lake Michigan Lobe area. *Illinois State Geol. Surv. Bull.*, 104.
- Hart, J.K. 1994. Till fabric associated with deformable beds. *Earth Surf. Process. Landf.*, **19**(1), 15–32.
- Hart, J.K. 1995. Subglacial erosion, deposition and deformation associated with deformable beds. *Progr. Phys. Geogr.*, **19**(2), 173–191.
- Hart, J.K. 2006. An investigation of subglacial processes at the microscale from Briksdalsbreen, Norway. *Sedimentology*, **53**(1), 125–146.
- Hart, J.K. and J. Rose. 2001. Approaches to the study of glacier bed deformation. *Quat. Int.*, **86**(1), 45–58.
- Hindmarsh, R.C.A. 1998a. Drumlinization and drumlin-forming instabilities: viscous till mechanisms. *J. Glaciol.*, **44**(147), 293–314.
- Hindmarsh, R.C.A. 1998b. The stability of a viscous till sheet coupled with ice flow, considered at wavelengths less than the ice thickness. *J. Glaciol.*, **44**(147), 285–292.
- Hobbs, B.E., W.D. Means and P.F. Williams. 1976. *An outline of structural geology*. New York, John Wiley and Sons.
- Hooke, R.LeB. and A. Elverhøi. 1996. Sediment flux from a fjord during glacial periods, Isfjorden, Spitsbergen. *Global Planet. Change*, **12**(1–4), 237–249.
- Hooyer, T.S. and N.R. Iverson. 2000a. Clast-fabric development in a shearing granular material: implications for subglacial till and fault gouge. *Geol. Soc. Am. Bull.*, **112**(5), 683–692.
- Hooyer, T.S. and N.R. Iverson. 2000b. Diffusive mixing between shearing granular layers: constraints on bed deformation from till contacts. *J. Glaciol.*, **46**(155), 641–651.
- Hooyer, T.S., N.R. Iverson, F. Lagroix and J.F. Thomason. 2008. Magnetic fabric of sheared till: a strain indicator for evaluating the bed deformation model of glacier flow. *J. Geophys. Res.*, **113**(F2), F02002. (10.1029/2007JF000757.)
- Iverson, N.R., B. Hanson, R.LeB. Hooke and P. Jansson. 1995. Flow mechanism of glaciers on soft beds. *Science*, **267**(5194), 80–81.
- Iverson, N.R., R.W. Baker and T.S. Hooyer. 1997. A ring-shear device for the study of till deformation: tests on tills with contrasting clay contents. *Quat. Sci. Rev.*, **16**(9), 1057–1066.
- Iverson, N.R., R.W. Baker, R.LeB. Hooke, B. Hanson and P. Jansson. 1999. Coupling between a glacier and a soft bed. I. A relation between effective pressure and local shear stress determined from till elasticity. *J. Glaciol.*, **45**(149), 31–40.
- Iverson, N.R. and 6 others. 2003. Effects of basal debris on glacier flow. *Science*, **301**(5629), 81–84.
- Iverson, N.R. and 7 others. 2007. Soft-bed experiments beneath Engabreen, Norway: regelation infiltration, basal slip and bed deformation. *J. Glaciol.*, **53**(182), 323–340.
- Iverson, N.R., T.S. Hooyer, J.F. Thomason, M. Graesch and J.R. Shumway. 2008. The experimental basis for interpreting particle and magnetic fabrics of sheared till. *Earth Surf. Process. Landf.*, **33**(4), 627–645.
- Jeffery, G.B. 1922. The motion of ellipsoidal particles immersed in a viscous fluid. *Proc. R. Soc. London, Ser. A*, **102**(715), 161–179.
- Jenson, J.W., P.U. Clark, D.R. MacAyeal, C. Ho and J.C. Vela. 1995. Numerical modeling of advective transport of saturated deforming sediment beneath the Lake Michigan lobe, Laurentide ice sheet. *Geomorphology*, **14**(2), 157–166.
- Jenson, J.W., D.R. MacAyeal, P.U. Clark, C.L. Ho and J.C. Vela. 1996. Numerical modeling of subglacial sediment deformation: implications for the behavior of the Lake Michigan lobe, Laurentide ice sheet. *J. Geophys. Res.*, **101**(B4), 8717–8728.
- Johnson, W.H. and A.K. Hansel. 1990. Multiple Wisconsinan glacial sequences at Wedron, Illinois. *J. Sediment. Petrol.*, **60**(1), 26–41.
- Johnson, W.H. and A.K. Hansel. 1999. Wisconsin Episode glacial landscape of central Illinois: a product of subglacial deformation processes? In Mickelson, D.M. and J.W. Attig, eds. *Glacial processes: past and present*. Boulder, CO, Geological Society of America, 121–135. (Special Paper 337.)
- Klein, E.C. and D.M. Davis. 2002. Surface sample bias and clast fabric interpretation based on till, Ditch Plains, Long Island. In Hanson, G.N., *Geology of Long Island and metropolitan New York*. New York, State University of New York. Long Island Geologists, 14–26.
- Koumoto, T. and K. Kaku. 1982. Three-dimensional analysis of static cone penetration into clay. In Verruijt, A., F.L. Beringen and E.H. de Leeuw, eds. *Penetration testing. Vol. 2*. Rotterdam, A.A. Balkema, 635–640.
- Larsen, N.K. and J.A. Piotrowski. 2003. Fabric pattern in a basal till succession and its significance for reconstructing subglacial processes. *J. Sediment. Res.*, **73**(5), 725–734.
- Larsen, N.K., J.A. Piotrowski and C. Kronborg. 2004. A multiproxy study of a basal till: a time-transgressive accretion and deformation hypothesis. *J. Quat. Sci.*, **19**(1), 9–21.
- Larsen, N.K., J.A. Piotrowski and J. Menzies. 2007. Microstructural evidence of low-strain, time-transgressive subglacial deformation. *J. Quat. Sci.*, **22**(6), 593–608.
- Lian, O.B., S.R. Hicock and A. Dreimanis. 2003. Laurentide and Cordilleran fast ice flow: some sedimentological evidence from Wisconsinan subglacial till and its substrate. *Boreas*, **32**(1), 102–113.
- Licciardi, J.M., P.U. Clark, J.W. Jenson and D.R. MacAyeal. 1998. Deglaciation of a soft-bedded Laurentide ice sheet. *Quat. Sci. Rev.*, **17**(4–5), 427–448.
- MacAyeal, D.R. 1992. Irregular oscillations of the West Antarctic ice sheet. *Nature*, **359**(6390), 29–32.
- Mark, D.M. 1973. Analysis of axial orientation data, including till fabrics. *Geol. Soc. Am. Bull.*, **84**(4), 1369–1373.
- Menzies, J., J.J.M. van der Meer and J. Rose. 2006. Till – as a glacial ‘tectomict’, its internal architecture, and the development of a ‘typing’ method for till differentiation. *Geomorphology*, **75**(1–2), 172–200.
- Murray, T. and G.K.C. Clarke. 1995. Black-box modeling of the subglacial water system. *J. Geophys. Res.*, **100**(B7), 10,231–10,245.
- Nicolas, A. 1992. Kinematics in magmatic rocks with special reference to gabbros. *J. Petrol.*, **33**(4), 891–915.
- Oertel, G. 1996. *Stress and deformation: handbook on tensors in geology*. New York, Oxford University Press.
- Ostry, R.C. and R.E. Deane. 1963. Microfabric analysis of till. *Geol. Soc. Am. Bull.*, **74**(2), 165–168.
- Piotrowski, J.A. and A.M. Kraus. 1997. Response of sediment to ice-sheet loading in northwestern Germany: effective stresses and glacier-bed stability. *J. Glaciol.*, **43**(145), 495–502.
- Piotrowski, J.A. and S. Tulaczyk. 1999. Subglacial conditions under the last ice sheets in northwest Germany: ice-bed separation and enhanced basal sliding? *Quat. Sci. Rev.*, **18**(6), 737–751.

- Piotrowski, J.A., D.M. Mickelson, S. Tulaczyk, D. Krzyszkowski and F.W. Junge. 2001. Were deforming subglacial beds beneath past ice sheets really widespread? *Quat. Int.*, **86**(1), 139–150.
- Piotrowski, J.A., N.K. Larsen and F.W. Junge. 2004. Reflections on soft subglacial beds as a mosaic of deforming and stable spots. *Quat. Sci. Rev.*, **23**(9–10), 993–1000.
- Principato, S.M., A.E. Jennings, G.B. Kristjánssdóttir and J.T. Andrews. 2005. Glacial-marine or subglacial origin of diamicton units from the southwest and north Iceland shelf: implications for the glacial history of Iceland. *J. Sediment. Res.*, **75**(6), 968–983.
- Stewart, R.A., D. Bryant and M.J. Sweat. 1988. Nature and origin of corrugated ground moraine of the Des Moines Lobe, Story County, Iowa. *Geomorphology*, **1**(2), 111–130.
- Stupavsky, M., D.T.A. Symons and C.P. Gravenor. 1974. Paleomagnetism of the Port Stanley Till, Ontario. *Geol. Soc. Am. Bull.*, **85**(1), 141–144.
- Tarling, D. and F. Hrouda. 1993. *Magnetic anisotropy of rocks*. London, Chapman and Hall.
- Thomason, J.F. 2006. Laboratory studies of till deformation with implications for the motion and sediment transport of the Lake Michigan Lobe. (PhD thesis, Iowa State University.)
- Thomason, J.F. and N.R. Iverson. 2006. Microfabric and microshear evolution in deformed till. *Quat. Sci. Rev.*, **25**(9–10), 1027–1038.
- Thomason, J.F. and N.R. Iverson. 2008. A laboratory study of particle ploughing and pore-pressure feedback: a velocity-weakening mechanism for soft glacier beds. *J. Glaciol.*, **54**(184), 169–181.
- Tikoff, B. and C. Teysier. 1994. Strain and fabric analyses based on porphyroclast interaction. *J. Struct. Geol.*, **16**(4), 477–491.
- Tulaczyk, S. 1999. Ice sliding over weak, fine-grained tills: dependence of ice–till interactions on till granulometry. In Mickelson, D.M. and J.W. Attig, eds. *Glacial processes: past and present*. Boulder, CO, Geological Society of America, 159–177. (Special Paper 337.)
- Van der Wateren, F.M., S.J. Kluiving and L.R. Bartek. 2000. Kinematic indicators of subglacial shearing. In Mickelson, D.M. and J.W. Attig, eds. *Glacial processes: past and present*. Boulder, CO, Geological Society of America, 159–177. (Special Paper 337.)
- Yi, C. and Z. Cui. 2001. Subglacial deformation: evidence from microfabric studies of particles and voids in till from the upper Ürümqi river valley, Tien Shan, China. *J. Glaciol.*, **47**(159), 607–612.

*MS received 25 February 2008 and accepted in revised form 17 August 2008*